https://doi.org/10.1016/j.cej.2021.132718

All-in-One and Bipolar-Membrane-Free Acid-Alkaline Hydrogel Electrolytes for Flexible High-Voltage Zn-Air Batteries

*Siyuan Zhao[a], Tong Liu[a***], Yawen Dai[a], Yang Wang[a], Zengjia Guo[a], Shuo Zhai[a],*

*Jie Yu[a], Chunyi Zhi[b**], Meng Ni[a*]*

[a] Building Energy Research Group, Department of Building and Real Estate, Research Institute for Sustainable Urban Development (RISUD) and Research Institute for Smart Energy (RISE), The Hong Kong Polytechnic University, Hung Hom, Kowloon, Hong Kong, China

[b] Department of Materials Science and Engineering, City University of Hong Kong, 83 Tat Chee Avenue, Kowloon 999077, Hong Kong, China

*Corresponding author

Email: meng.ni@polyu.edu.hk, cy.zhi@cityu.edu.hk, tongliu@polyu.edu.hk

Table of Contents

A novel all-in-one and bipolar-membrane-free hydrogel electrolyte is designed for flexible high-voltage Zn-Air batteries (ZABs). The battery exhibits an unprecedentedly high voltage of 2 V, surpassing all the reported flexible ZABs.

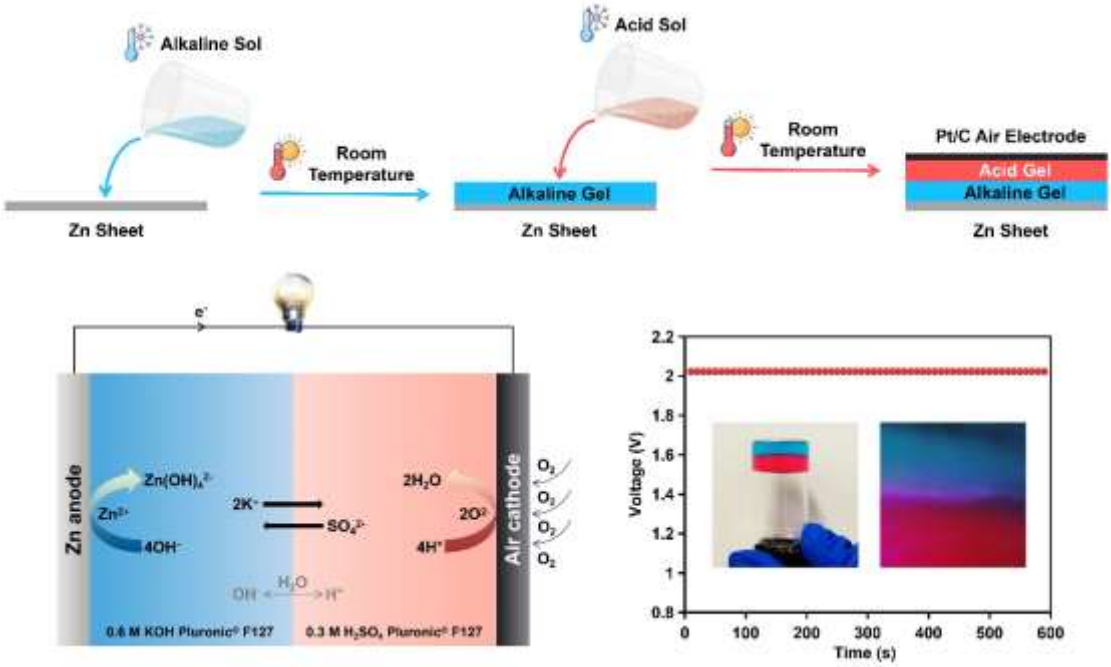

Highlights

- An All-in-one and membrane-free acid-alkaline hydrogel electrolyte is proposed.
- A simplified structure with intimate electrode-electrolyte interface is achieved.
- The fabricated flexible ZAB exhibits an unprecedentedly high voltage of 2 V.
- The “two flavors in one meat” design is available for other dual-electrolyte batteries.

Abstract

The low operating voltage of 1.4 V limits the widespread application of flexible Zn-air batteries (ZABs) in wearable electronics. However, a high-voltage flexible ZAB has not been achieved yet, which results from the few choices of fitted flexible electrolytes. Now we propose a novel, universal, and simple strategy to design all-in-one and membrane-free acid-alkaline flexible electrolytes based on thermo-reversible Pluronic® F127 hydrogels. Benefiting from the unique sol-gel transition property of Pluronic® F127 hydrogel, the acid and alkaline can be decoupled but integrated simultaneously in one hydrogel. Surprisingly, the as-developed ZAB achieves an unprecedentedly high voltage of 2 V, surpassing all the existing flexible ZABs. Meanwhile, this battery exhibits remarkable high-voltage stability of 37 hours and a large area capacity of 1.35 mAh cm^{-2} without the use of costly bipolar membranes. Our work presents a pioneering example for flexible high-voltage ZAB and may further inspire other designs of flexible high-voltage aqueous batteries and decoupled dual-electrolyte batteries.

Keywords: acid-alkaline electrolyte, all-in-one, high-voltage, hydrogel electrolyte, thermo-reversible hydrogel, zinc-air battery

Introduction

Flexible aqueous Zn-based batteries with hydrogel electrolytes are ideal power sources for wearable electronic devices owing to their intrinsic safety and low cost [1-5]. Among them, flexible ZABs are especially outstanding and attract tremendous interest for their high theoretical energy density (1084 Wh kg^{-1}) and stable discharge platforms [6, 7]. Regretfully, they deliver a low operating voltage of 1.4 V because of their low cathodic potential in alkaline environments, which lowers the battery energy density and limits their widespread application [8-11]. Therefore, there is an urgent need to develop flexible high-voltage ZABs; however, which have not been reported yet.

Recently, the voltage of liquid-state ZABs was successfully elevated to over 2 V by decoupling the liquid electrolyte into acid catholyte and alkaline anolyte, separated by a bipolar membrane for preventing neutralization [12, 13]. This way, the Zn anode can retain stability in alkaline, and the air cathode in acid exhibits a higher potential [14, 15]. The following reactions explained for the voltage promotion:

Anode in alkaline anolyte:

$$Zn + 4OH^- = Zn(OH)_4^{2-} + 2e^- \qquad E^\theta = -1.199 \text{ V vs SHE}$$

Cathode in alkaline catholyte:

$$O_2(g) + 2H_2O + 4e^- = 4OH^- \qquad E^\theta = 0.401 \text{ V vs SHE}$$

Cathode in acid catholyte:

$$O_2(g) + 4H^+ + 4e^- = 2H_2O \qquad E^\theta = 1.229 \text{ V vs SHE}$$

For conventional flexible sandwich-structure ZABs (**Figure 1a**), the self-standing hydrogel electrolyte is employed to replace the liquid-state alkaline electrolyte to achieve battery flexibility [16-18]. Inspired by the double-meat sandwich (**Figure 1b**), it is theoretically feasible to pile up the individual acid and alalkaline hydrogel electrolytes, which directly applies the acid-alkaline decoupling strategy from liquid-state ZABs to achieve flexible high-voltage solid-state ZABs [19]. However, ZABs with this cumbersome multiple-layer structure may easily delaminate during repeated daily bending, leading to increased resistance at the electrode-electrolyte and electrolyte-electrolyte interfaces, even battery performance degradation [20, 21]. Moreover, the use of bipolar membrane inevitably increases the battery cost and further complicates the battery structure [22]. Hence, there should be a transformative shift on hydrogel electrolyte design for flexible high-voltage batteries but very challenging.

Herein, for the first time, we develop a novel "two flavors in one meat" structure (**Figure 1c**), that is, an all-in-one and membrane-free acid-alkaline hydrogel electrolyte (AAHE) based on a thermo-reversible Pluronic® F127 hydrogel. By virtue of the unique sol-gel transition property of Pluronic® F127 hydrogel, the acid and alkaline can be decoupled but integrated simultaneously in one hydrogel and maintain high stability, thus avoiding the use of an expensive bipolar membrane. Furthermore, this all-in-one design dramatically simplifies the multiple-layer structure and contributes to integrated electrolyte-electrolyte and electrode-electrolyte interfaces. Surprisingly, the fabricated flexible ZABs exhibited an unprecedented high voltage of 2 V, surpassing all the existing flexible ZABs. Meanwhile, this battery exhibits remarkable high-voltage

stability of 37 hours and a large area capacity of 1.35 mAh cm^{-2}.

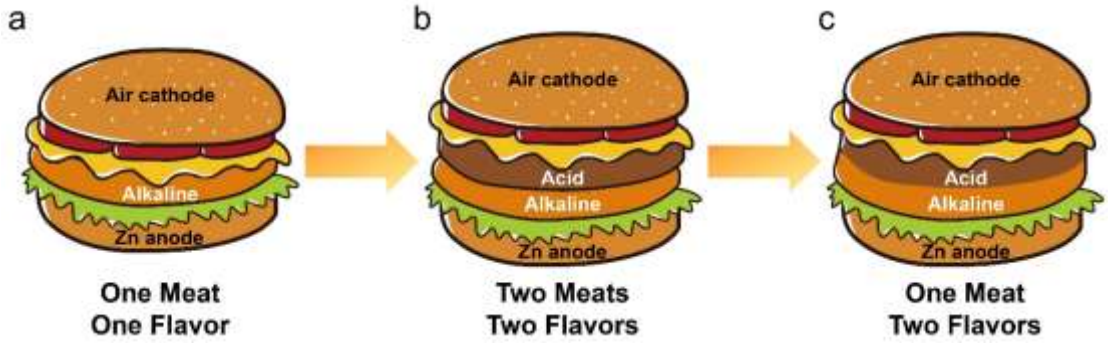

Figure 1. The evolution process of sandwiches from (a) conventional structure → (b) recent double-meat structure with two flavors → (c) novel "two flavors in one meat" structure, which demonstrated the design strategy of the flexible high-voltage ZAB with all-in-one and membrane-structure AAHE.

Experimental Section

Materials: Potassium hydroxide (85%, pellets), sulfuric acid (98%, liquid), potassium sulfate (99%, powder), zinc sulfate heptahydrate (99%, powder), Copper(II) sulfate pentahydrate (98%, powder), Sodium stannate trihydrate (95%, powder), and Pluronic® F127 (PEO_{100}-PPO_{65}-PEO_{100}, Critical Micelle Concentration (CMC): 950-1000 ppm, powder) for preparing hydrogel electrolytes were purchased from SIGMA-ALDRICH. The dye Congo Red (Dye content 35%, powder) and Methylene Blue (Dye content 82%, powder) used for dyeing red and blue, respectively, are also bought from SIGMA-ALDRICH. PVA (molecular weight of 195000, powder) was purchased from Aladdin. Zinc electrode (thickness of 0.1 mm), copper electrode (thickness of 0.2 mm), aluminum electrode (thickness of 0.2 mm), were purchased from Changsha Spring Corporation. Carbon paper, carbon cloth, and 20% Pt/C catalyst were bought from

Shanghai Hesen Corporation. Deionized water was used throughout the experiments. All the materials were used as received.

Preparation of Pluronic® F127 hydrogel electrolytes: Pluronic® F127 is a triblock copolymer which can dissolve in water and become gel-state by micellization. Taking the alkaline Pluronic® F127 hydrogel electrolyte for example, at room temperature, 30 wt% Pluronic® F127 powders were added into 0.6 M KOH solution (alkaline part of AAHE for flexible ZABs) in sealed glass vials. To obtain transparent and uniform hydrogel electrolytes, the suspension solution was first placed at -10 ℃ for 12 hours until F127 powders completely dissolving in KOH solution and then placed the obtained transparent solution at room temperature for 30 minutes. For other hydrogel electrolytes, the 0.6 M KOH solution can be replaced by DI water (pristine Pluronic® F127), 0.6 M KOH + 0.01 M Na_2SnO_3 (alkaline part of AAHE for flexible AABs), 0.3 M H_2SO_4 (acid part of AAHE for flexible ZABs and AABs), 0.1 M K_2SO_4 (neutral layer of ANAHE for flexible ZABs), 0.5 M $ZnSO_4$ (Zn part of the decoupled electrolyte for flexible Zn-Cu batteries), 0.5 M $CuSO_4$ (Cu part of the decoupled electrolyte for flexible Zn-Cu batteries). The red acid Pluronic® F127 and blue alkaline Pluronic® F127 are dyed by adding 0.1 wt% Congo Red and 0.1 wt% Methylene Blue into the corresponding solution, respectively.

Preparation of PVA hydrogel electrolytes: Taking the alkaline PVA hydrogel electrolyte for example, 1 g PVA powders were dissolved in 10 mL 0.6 M KOH solution at 90 ℃ under magnetic stirring for an hour. Then, this high-viscosity solution was placed in a refrigerator at -20 ℃ for 24 hours. After that, the freezing PVA was taken

out and thawed at room temperature. The freezing-thawing process was repeated for 3 times to obtain a self-standing alkaline PVA hydrogel. For acid PVA hydrogel, the 0.6 M KOH solution was replaced by 0.3 M H_2SO_4. The red acid PVA and blue alkaline PVA are dyed by adding 0.1 wt% Congo Red and 0.1 wt% Methylene Blue into the corresponding solution, respectively.

Fabrication of the flexible decoupled electrolyte batteries: Taking the AAHE-based ZAB for example, cold sol-state alkaline was poured on the Zn surface to form a conformal interface. Then, after the sol-state alkaline transforming to a gel state at room temperature, cold sol-state acid was poured on the gel-state alkaline with a 2 mg cm^{-2} loading Pt/C air electrode on the top. Finally, the sol-state acid transformed to gel state at room temperature. This fabrication process could also apply to AABs, Zn-Cu batteries, and other kinds of decoupled electrolyte batteries.

Characterization and electrochemical detection: FTIR was conducted by a PerkinElmer Spectrum in ATR mode scanning from 3600 to 600 cm^{-1}. XRD was conducted by Rigaku smartlab ranging from 5° to 75°. Hydrogel sol-gel transition temperatures were measured by DSC (TA Instrument Inc). Hydrogel viscosities were obtained using a rheometer (HAAKE, MARS4) performing at 25 ℃ with an angular frequency of 6.283 rad/s. The electrolyte-electrolyte and electrode-electrolyte contact were observed by a digital microscope (Sanqtid). A scanning electron microscope (SEM, HITACHI, S-4800) was used to observe the Pt/C loaded air electrode and Al surface. For the water retention capacity evaluation, hydrogels were placed without any coverage at 25 ℃ and relative humidity (RH) of 60 %. The weight retention was

calculated by $W_{certain\ time}/W_{initial}$. The AC impedance spectra of the ZAB and hydrogel electrolytes were measured in the frequency range of 0.01–100000 Hz with a magnitude of 10 mV (at OCV) using CHI660E electrochemical workstation. The Linear sweep voltammetry (LSV) were conducted at a scanning rate of 1 mV s^{-1} (CHI660E) for AAHE's electrochemical stability window curves and ZAB's polarization curves. Neware battery testing system was used in this work to test the battery discharge performance. It should be noted that AAHE and PVA hydrogels related experiments are conducted at as-prepared gel-state without freeze-drying.

Results and Discussion

The reported ZAB is composed of a Zn anode, an Pt/C air cathode, and the key for battery flexibility and high voltage, the newly developed AAHE (**Figure 2a**) [23, 24]. Unlike the widely used self-standing hydrogels (e.g., polyvinyl alcohol, abbr. PVA), AAHE is made of thermo-reversible Pluronic® F127 hydrogels which are sol state at subzero temperature but transform to viscous gel state at room temperature (**Figure 2b**) [25]. Take advantage of this unique sol-gel transition property, the flexible high-voltage ZAB can be facilely fabricated as demonstrated in **Figure 2c**: First, the cold sol-state alkaline Pluronic® F127 is poured on the Zn surface to form a conformal interface. After transforming to a gel-state alkaline Pluronic® F127 at room temperature, the cold sol-state acid Pluronic® F127 is poured on it with a fully contacted air cathode on the top. Finally, the sol-state acid Pluronic® F127 soon transforms to gel-state acid Pluronic® F127 at room temperature. Within this fabrication process, the acid and alkaline are also decoupled but integrated to form an unprecedented all-in-one and membrane-free acid-

alkaline hydrogel electrolyte (**Figure 2d**).

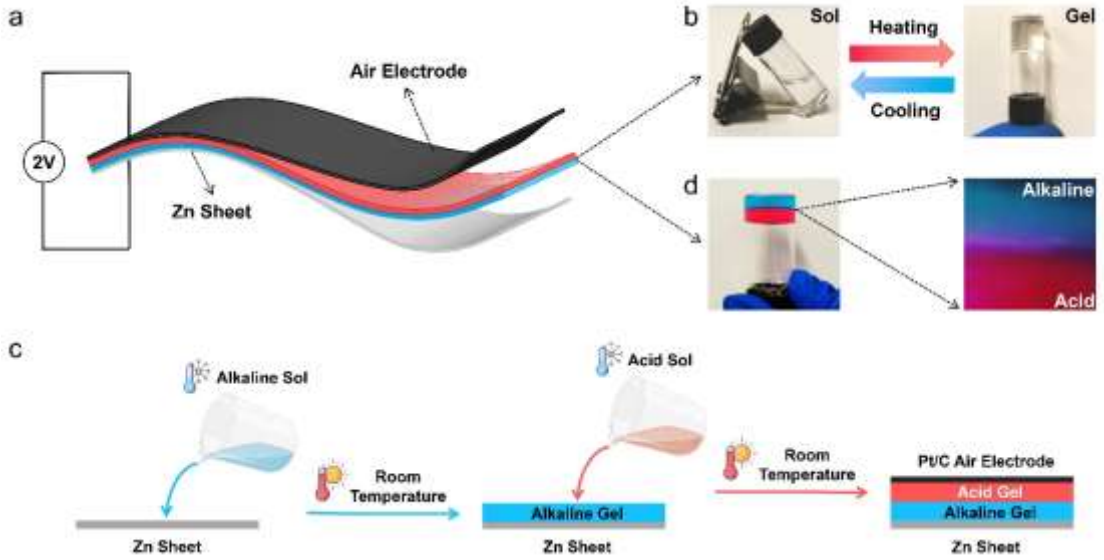

Figure 2. (a) Schematic of the flexible high-voltage ZAB. (b) Sol-gel transition property of the AAHE component Pluronic® F127. (c) Fabrication process of the AAHE-based ZAB: Cold sol-state alkaline is poured on the Zn surface to form a conformal interface → After transforming to a gel-state alkaline at room temperature, cold sol-state acid is poured on it, followed by an air electrode on the top → Return to room temperature for a gel-state acid. (d) All-in-one and membrane-free structure of AAHE with an integrated electrolyte-electrolyte interface.

Further characterizations are conducted for a better understanding of the physicochemical properties of AAHE. Pristine, acid, and alkaline Pluronic® F127 hydrogels are prepared for testing under their original hydrogel state without freeze-drying. The broad peaks detected among 3600 to 3100 cm^{-1} in the FTIR spectra are the O-H stretching band (**Figure 3a**). From 3100 to 2600 cm^{-1}, the observed peaks are the C-H stretching. Moreover, peaks arising at 1080 and 945 cm^{-1} in the FTIR spectra

represent the C-O-C and C-OH stretching in Pluronic® F127, respectively (**Figure 3a**). The peaks of the acid and alkaline Pluronic® F127 hydrogels are consistent with the pristine Pluronic® F127 hydrogel, indicating their successful synthesis and the fact that acid and alkaline will not change the chemical structure of Pluronic® F127. No peak is shown in the pristine, acid, and alkaline Pluronic® F127 hydrogels' XRD patterns, demonstrating AAHE is an amorphous gel state (**Figure 3b**). Besides, the nearly same XRD results confirm that the acid and alkaline will not affect the gel-state of Pluronic® F127. To further reveal the specific sol-gel transition temperatures of AAHE, differential scanning calorimetry (DSC) is conducted. As shown in **Figure 3c**, the acid and alkaline parts of AAHE both enjoy a low sol-gel transition temperature of -2.88 and -4.25 ℃, respectively, while the pristine Pluronic® F127 is much higher as 14.08 ℃. This is because the existence of salt can lower the sol-gel transition temperature significantly, which is consistent with our previous report [25]. Besides, further DSC measurement indicates AAHE retaining highly thermo-stable by 100 ℃, ensuring a wide working range for ZABs (**Figure S1**). On the other hand, both pristine and AAHE exhibit a high viscosity (~10^7 times the liquid water, **Figure 3d**), which effectively alleviates the mixing of decoupled acid and alkaline [26, 27]. Thus, AAHE and ZABs can retain high stability without the use of a bipolar membrane. Moreover, the high viscosity also indicates the good mechanical strength of AAHE, which is critical for ZABs to be both robust and flexible.

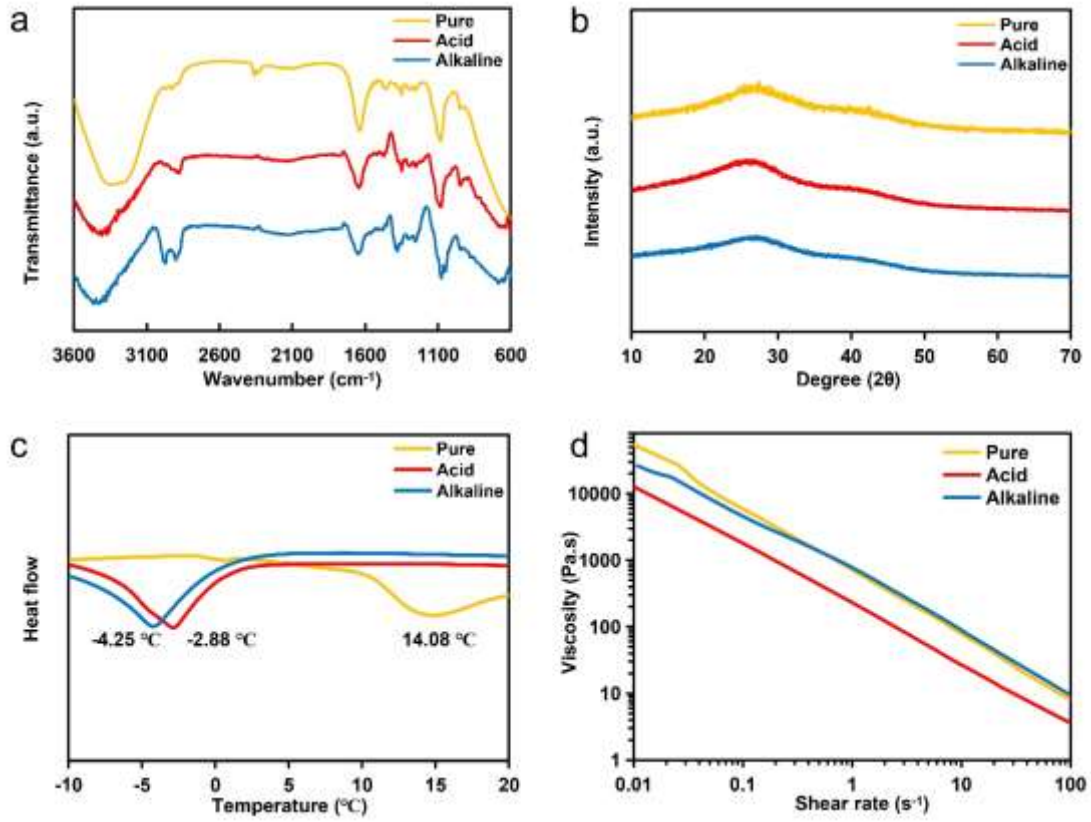

Figure 3. (a) FTIR spectra, (b) XRD patterns, (c) DSC curves, and (d) viscosities of the pristine Pluronic® F127 and the acid and alkaline part of AAHE.

The application of AAHE further simplifies the multi-layer battery structure and avoids the battery delamination. To highlight the advantages of AAHE, conventional self-standing crosslinked PVA hydrogels are used for comparison [28, 29]. As shown in **Figure 4a**, AAHE exhibits an all-in-one and membrane-free structure with an integrated interface. However, distinct void can be observed on the double-layer acid and alkaline PVA interface (**Figure 4d**). Besides, benefiting from the sol-state below the transition temperature, AAHE obtains intimate contacts between both Zn anode and air cathode (**Figure 4b and c**). The *in situ* gelation on the electrode surface guarantees the battery structure stability during daily bending [30]. Nevertheless, both acid and

alkaline PVA hydrogel electrolytes show loose contacts at electrode-electrolyte interfaces, which leads to the bulky multiple-layer battery structure and may easily cause battery delamination (**Figure 4e and f**) [31]. More importantly, these interfacial contacts are highly related to battery electrochemical performances [32]. The poor contact between acid and alkaline PVA greatly increases the interfacial resistance. As a result, the ionic conductivity of the acid-alkaline PVA decreases significantly compared with individual acid or alkaline PVA hydrogel electrolytes (75 to 27 mS cm^{-1}) (**Figure 4g and S2**). However, the ionic conductivities of the individual acid and alkaline Pluronic® F127 and AAHE retain consistency as high as 26 mS cm^{-1} (**Figure 4g and S2**). This phenomenon is attributed to the integrated electrolyte-electrolyte interface of AAHE, where no additional interfacial resistance is produced. They have outperformed many other reports though sacrificed compared to the ionic conductivities of the liquid acid and alkaline (**Figure S3**) [33-35]. The activation energy can tell the ease of ion transport within AAHE. Therefore, the ionic conductivities of AAHE at various temperatures are measured. As shown in **Figure S4**, the ionic conductivity increases with the temperature rising, and low activation energy of 11.54 KJ mol^{-1} is calculated by the Arrhenius plot. On the other hand, the conformal contacts between AAHE and electrodes contribute to a lower charge transfer resistance (R_{ct}) than PVA hydrogel electrolyte, reflected in the smaller semicircle in the AC impedance spectra (**Figure 4h**).

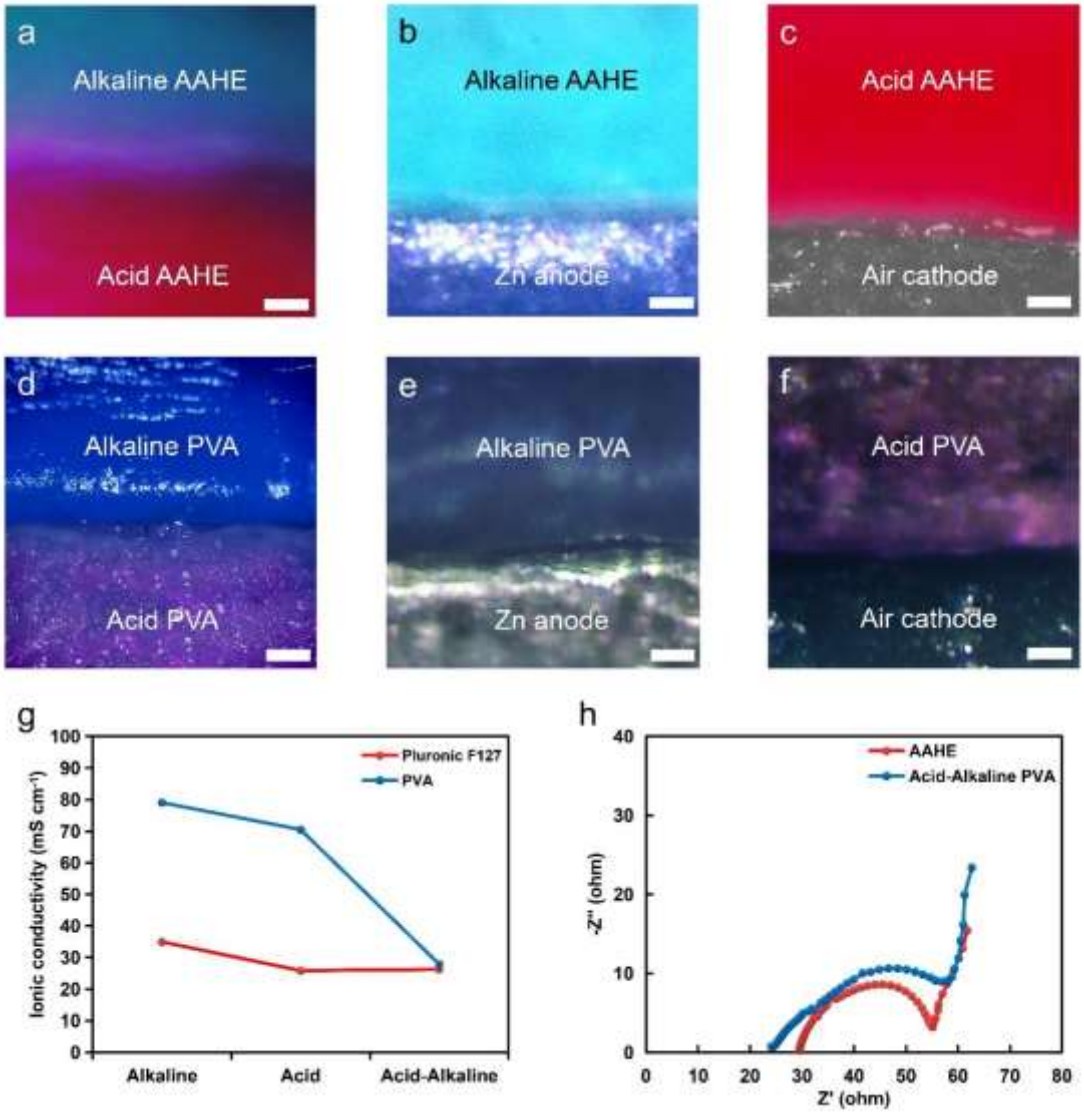

Figure 4. Microscope images of the integrated interface of (a) all-in-one AAHE, (b) alkaline part of AAHE and Zn anode, (c) acid part of AAHE and air cathode; and the loose contact between (d) alkaline and acid PVA, (e) alkaline PVA and Zn anode, (f) acid PVA and air cathode. (g) Ionic conductivities of the acid, alkaline, acid-alkaline Pluronic® F127 and PVA. (h) AC impedance of the AAHE and acid-alkaline PVA based ZABs. Scale bar: 50 μm.

Figure 5 demonstrates the ion transport behavior within the AAHE-based ZABs. During discharge, OH^- react with the oxidized Zn anode (Zn^{2+}) and become $Zn(OH)_4^{2-}$

in the alkaline part of AAHE. On the other side, oxygen in the air is reduced by the air cathode to become O^{2-}, which combine with H^+ to produce water. The decoupled reactions in alkaline and acid environments maximize the potential gap between zinc anode and air cathode. Meanwhile, the cation K^+ and anion SO_4^{2-} shuttle through AAHE while the electrons transport from anode to cathode by external circuit. Since there is no bipolar membrane in AAHE, the acid-alkaline neutralization is unavoidable. Luckily, the high viscosity of AAHE significantly alleviates this process.

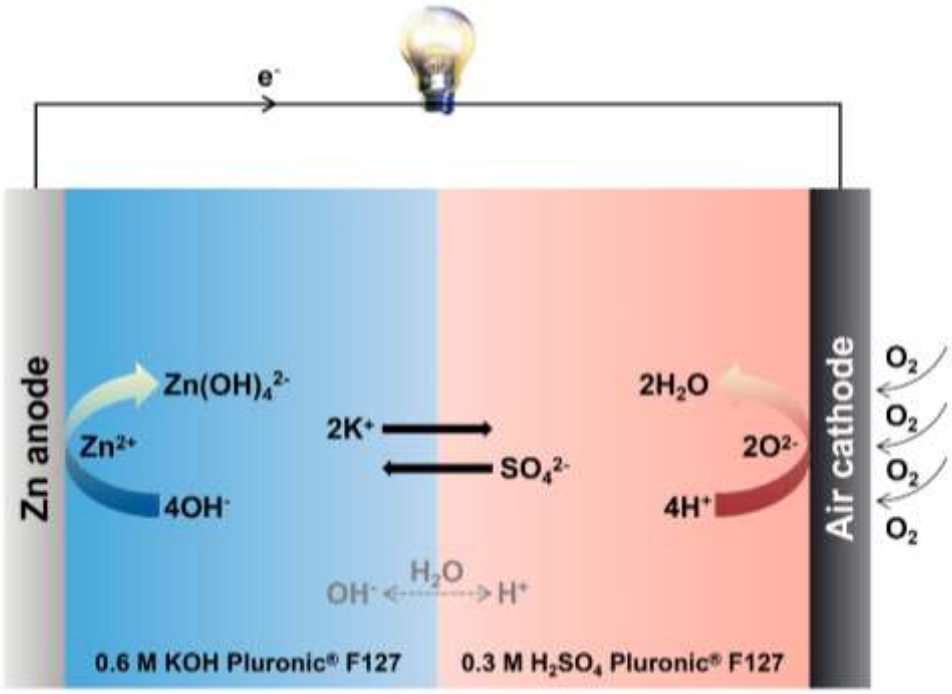

Figure 5. Schematic of the ion transport behavior within AAHE-based ZABs.

The Pt/C air electrode is used as a stable exemplary model in an acid environment (**Figure S5**) [36]. On the other hand, AAHE exhibits a wide electrochemical stability window of ~ 2.75 V, which guarantees electrolyte stability under high voltage (**Figure S6**). By virtue of these, the fabricated ZAB exhibits an unprecedentedly high open-circuit voltage (OCV) of 2.02 V, which gains an increment of 0.61 V (~43%) compared

to the conventional alkaline normal-voltage ZAB (**Figure 6a**). The discharge voltage at 0.1 mA cm^{-2} is also increased by ~52% from 1.26 to 1.91 V (**Figure 6b**). It is the first time to elevate the voltage to over 2 V among all the reported flexible ZABs with various hydrogel electrolytes, including the widely used gelatin, PVA, polyacrylamide (PAM), polyacrylic acid (PAA), and sodium polyacrylate (PANa) hydrogels (**Figure 6c** and **Table S1**) [35, 37-40]. The increment in voltage also brings about a higher battery power density. As shown in **Figure 6d**, the power density of the AAHE-based ZAB rises to 4.2 mW cm^{-2}, which is increased by 20% than the conventional alkaline normal-voltage ZAB with 3.5 mW cm^{-2}. The water retention capacity of the hydrogel electrolyte is crucial for a long-duration battery operation. The loss of water will lead to a severe hydrogel shrinkage and decrease in ionic conductivity, collapsing the battery structure and degrading the battery performance [41, 42]. Impressively, AAHE exhibits high water retention of ~93% after 48 hours, while the counterpart PVA hydrogel can only retain ~23% (**Figure S7**). This may be due to the strong interaction between water molecules and hydrophilic PEO chains and the water restriction effect provided by the hydrophobic PPO chains within AAHE [43]. Moreover, the high viscosity of AAHE restrains the acid-alkaline neutralization and further facilitates the long-term operation of our high-voltage ZAB. As a result, this battery exhibits a remarkably stable and high OCV (~2 V) with an ultra-long duration of 37 hours, greatly surpassing the 9 hours of the ZAB with an acid-alkaline PVA hydrogel electrolyte (**Figure 6e**). Besides, the AAHE-based ZAB can also discharge for 13.5 hours at 0.1 mA cm^{-2} with a stable high-voltage platform, while the PVA-based ZAB fails after 3.5 hours discharge (**Figure 6f**).

The end of discharge can be explained by the gradual consumption of H^+ and OH^- within AAHE during the half-reaction on both cathode and anode. For further validation, we change both the used zinc anode and air cathode with new ones and remain the exhausted AAHE. As expected, the reassembled ZAB obtains a low beginning voltage and exhibits no discharge ability (**Figure S8**). Furthermore, the sol-gel transition temperatures of both the acid and alkaline parts of AAHE increase slightly after discharging (**Figure S9**). According to our previous research, this phenomenon is due to the decrease in acid and alkaline concentration, which further proves our explanation for battery failure [25]. The AAHE-based ZAB also exhibits a good rate performance when discharging at different current densities. As shown in **Figure 6g**, the battery delivers a large area capacity of ~1.35 mAh cm^{-2} at 0.1 and 0.2 mA cm^{-2}. The area capacity also maintains over 1 mAh cm^{-2} at a higher current density of 0.5 mA cm^{-2} (**Figure 6g**).

In liquid-state acid-alkaline batteries, a neutral chamber is employed to separate the acid and alkaline for a longer battery operation [44, 45]. Here, following the similar steps in **Figure 2c**, we further present a "three flavors in one meat" acid-neutral-alkaline hydrogel electrolyte (ANAHE) for ZABs. However, the ZABs with AAHE and ANAHE deliver a comparable OCV duration, where the effect of the neutral layer is not evident (**Figure S10**). This is because the neutral layer is more like a buffer layer to prevent the direct contact between the acid and alkaline part of AAHE. However, the neutral layer cannot serve as a bipolar membrane which completely inhibits the free move of H^+ and OH^- ions (**Figure S11**). Besides, the neutral layer increases the

resistance of ANAHE, which leads to a decline in battery discharge voltage (**Figure S12**) [46]. Therefore, AAHE with better performances and a simpler structure is more suitable for flexible high-voltage ZABs.

An encapsulation-free structure with slight voltage sacrifice is further used for battery flexibility presentations. **Figure 6h** demonstrates the impressive discharge stability of the flexible AAHE-based ZAB under a 60° bending state. Even after 100 times bending and back to planar state, the battery shows no structure delamination, and the discharge profile hardly changes, illustrating the decisive role of AAHE in battery stability (**Figure 6h**). By virtue of the high voltage, one single bending-state AAHE-based ZAB can light up a series LED while the conventional alkaline normal-voltage ZAB cannot (**Figure 6i**), manifesting the practical significance of the high-voltage ZABs.

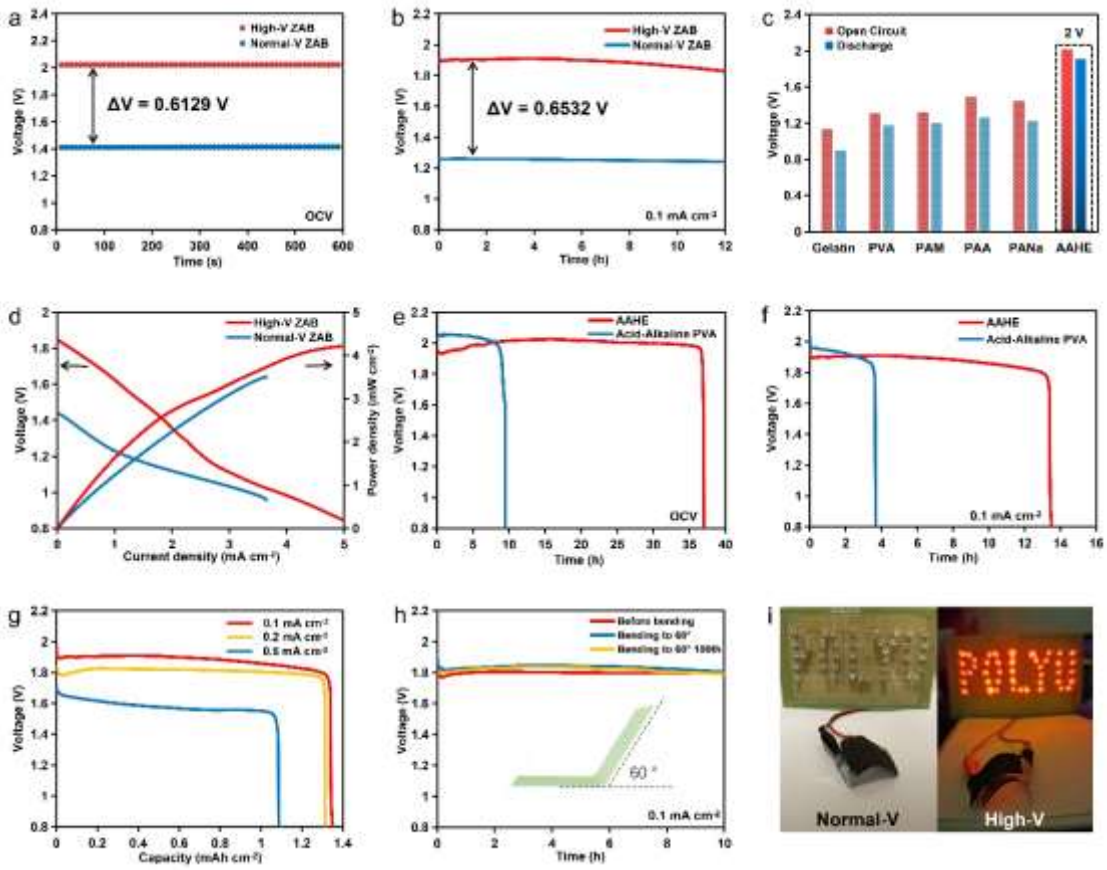

Figure 6. Comparison of (a) OCV and (b) 0.1 mA cm^{-2} discharge profiles between the AAHE-based high-voltage and conventional alkaline normal-voltage ZABs. (c) Voltage comparison of different hydrogel-based flexible ZABs. (d) Polarization and power density profiles of the AAHE-based high-voltage ZAB and conventional alkaline Pluronic® F127 based normal-voltage ZAB. Comparison of (e) OCV and (f) 0.1 mA cm^{-2} discharge profiles between the AAHE and acid-alkaline PVA based ZABs. (g) Discharge profiles of the AAHE-based ZABs at different current densities. (h) Discharge profiles of the AAHE-based ZABs before and at 60° bending state, and after 100 times 60° bending back to planar. The inner schematic shows the 60° bending state. (i) One single bending-state high-voltage ZAB (right) lighting up a series LED while the conventional alkaline normal-voltage ZAB incapable (left).

Furthermore, AAHE is universal for other kinds of metal-air batteries like Al-air batteries (AABs). As shown in **Figure 7a and b**, the OCV and discharge voltage of the AAHE-based AABs both increase significantly compared to the conventional alkaline AABs. The gradually decreasing discharge voltage is due to the passivation on the Al surface, rather than the degradation of AAHE (**Figure S13**) [47]. In the future, the "two flavors in one meat" design strategy can be further applied to generalized flexible decoupled dual-electrolyte batteries and it has been confirmed successful in the flexible Zn-Cu batteries with $ZnSO_4$ and $CuSO_4$ electrolytes. Since there is no neutralization in the Zn-Cu battery, it preserves an ultra-stable OCV for over 200 hours and a long discharge duration for about 150 hours (**Figure 7c and d**).

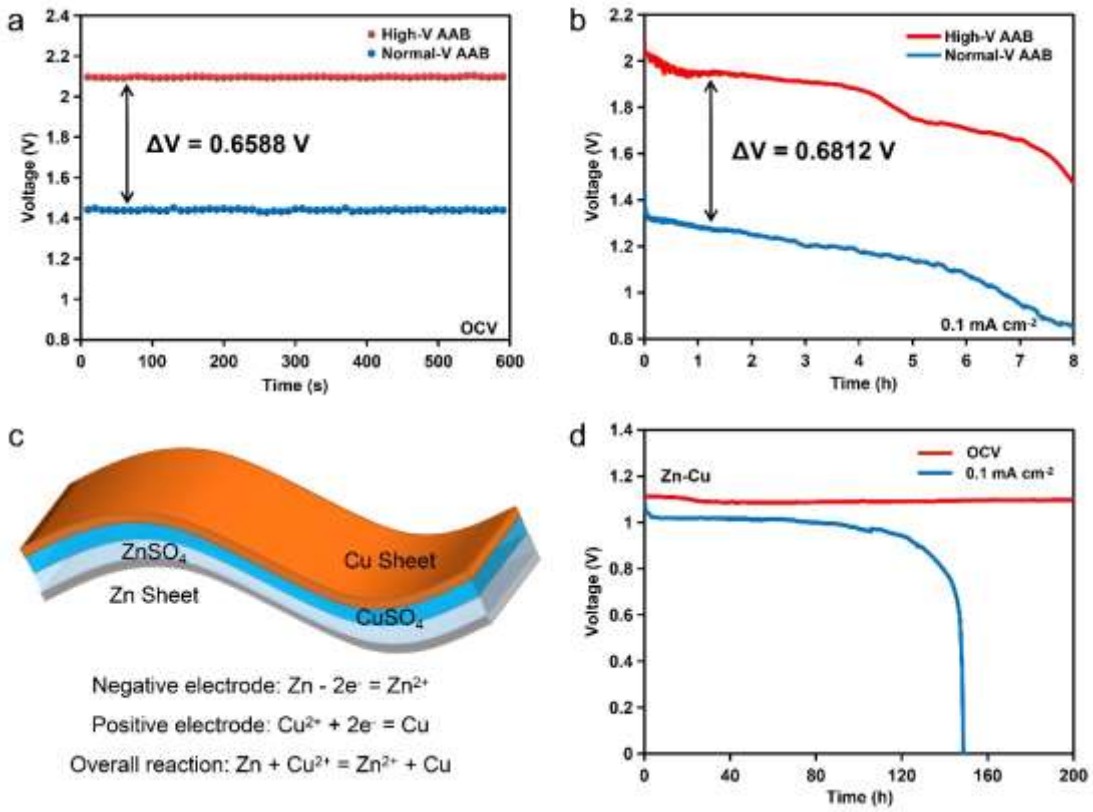

Figure 7. Comparison of (a) OCV and (b) 0.1 mA cm^{-2} discharge profiles between the AAHE-based high-voltage and conventional alkaline normal-voltage AABs. (c) Schematic of the flexible Zn-Cu battery with $ZnSO_4$-$CuSO_4$ decoupled dual-electrolyte. (d) OCV and 0.1 mA cm^{-2} discharge profiles of the flexible Zn-Cu battery.

Conclusion

In summary, we propose a novel, simple, universal, and effective "two flavors in one meat" strategy to design acid-alkaline hydrogel electrolytes for flexible ZABs, which achieve an unprecedentedly high voltage of 2 V and large area capacity of 1.35 mAh cm^{-2}. The all-in-one and membrane-free structure of AAHE significantly simplify the battery structure, and intimate contacts between AAHE and electrodes further contribute to the battery stable discharge even after multiple times bending. Moreover,

the AAHE design strategy can be further extended to other batteries with decoupled dual-electrolyte. In the future, more efforts should focus on increasing the concentration of AAHE for a better battery performance. Cathode with high activity and stability towards oxygen reduction/evolution reaction in the acid environment is also crucial for battery rechargeability.

Conflict of Interest

The authors declare no competing financial interest.

Author Contributions

Siyuan ZHAO: Conceptualization, Methodology, Investigation, Writing original draft, Supervision. **Tong LIU:** Investigation, Writing-review & editing, Supervision. **Yawen DAI:** Investigation, Validation. **Yang WANG:** Validation. **Zengjia GUO:** Investigation. **Shuo ZHAI:** Validation. **Jie YU:** Validation. **Chunyi ZHI:** Writing-review & editing, Supervision. **Meng NI:** Funding acquisition, Writing-review & editing, Supervision.

Acknowledgement

This work is supported by a grant from Collaborative Research Fund (CRF) (Project no. C5031-20G) of Research Grant Council, University Grant Committee, HK SAR. We also thank the help from Dr. Jinhye Bae, Jiayu Zhao, and Minghao Li from University of California, San Diego.

Reference

[1] Y. Guo, J. Bae, Z. Fang, P. Li, F. Zhao, G. Yu, Hydrogels and Hydrogel-Derived Materials for Energy and Water Sustainability, Chem. Rev. 120(15) (2020) 7642-7707.
[2] C.Y. Chan, Z. Wang, H. Jia, P.F. Ng, L. Chow, B. Fei, Recent advances of hydrogel electrolytes in flexible energy storage devices, Journal of Materials Chemistry A 9(4) (2021) 2043-2069.
[3] Z. Wang, H. Li, Z. Tang, Z. Liu, Z. Ruan, L. Ma, Q. Yang, D. Wang, C. Zhi, Hydrogel Electrolytes for Flexible Aqueous Energy Storage Devices, Adv. Funct. Mater. 28(48) (2018) 1804560.
[4] M. Chen, J. Chen, W. Zhou, X. Han, Y. Yao, C.P. Wong, Realizing an All-Round Hydrogel Electrolyte toward Environmentally Adaptive Dendrite-Free Aqueous Zn–MnO2 Batteries, Adv. Mater. 33(9) (2021) 2007559.
[5] M. Chen, W. Zhou, A. Wang, A. Huang, J. Chen, J. Xu, C.-P. Wong, Anti-freezing flexible aqueous Zn–MnO2 batteries working at −35 °C enabled by a borax-crosslinked polyvinyl alcohol/glycerol gel electrolyte, Journal of Materials Chemistry A 8(14) (2020) 6828-6841.
[6] Y. Wei, Y. Shi, Y. Chen, C. Xiao, S. Ding, Development of solid electrolytes in Zn–air and Al–air batteries: from material selection to performance improvement strategies, Journal of Materials Chemistry A 9(8) (2021) 4415-4453.
[7] Y. Zhang, Y.-P. Deng, J. Wang, Y. Jiang, G. Cui, L. Shui, A. Yu, X. Wang, Z. Chen, Recent Progress on Flexible Zn-Air Batteries, Energy Storage Materials 35 (2021) 538-549.
[8] P. Pei, S. Huang, D. Chen, Y. Li, Z. Wu, P. Ren, K. Wang, X. Jia, A high-energy-density and long-stable-performance zinc-air fuel cell system, Applied Energy 241 (2019) 124-129.
[9] L. Li, A. Manthiram, Long-Life, High-Voltage Acidic Zn–Air Batteries, Advanced Energy Materials 6(5) (2016) 1502054.
[10] X. Yuan, X. Wu, X.X. Zeng, F. Wang, J. Wang, Y. Zhu, L. Fu, Y. Wu, X. Duan, A fully aqueous hybrid electrolyte rechargeable battery with high voltage and high energy density, Advanced Energy Materials 10(40) (2020) 2001583.
[11] F. Yu, L. Pang, X. Wang, E.R. Waclawik, F. Wang, K.K. Ostrikov, H. Wang, Aqueous alkaline–acid hybrid electrolyte for zinc-bromine battery with 3V voltage window, Energy Storage Materials 19 (2019) 56-61.
[12] Y. Ding, P. Cai, Z. Wen, Electrochemical neutralization energy: from concept to devices, Chem. Soc. Rev. (2021).
[13] C. Lin, S.-H. Kim, Q. Xu, D.-H. Kim, G. Ali, S.S. Shinde, S. Yang, Y. Yang, X. Li, Z. Jiang, High-voltage asymmetric metal–air batteries based on polymeric single-Zn2+-ion conductor, Matter 4(4) (2021) 1287-1304.
[14] J. Hao, X. Li, X. Zeng, D. Li, J. Mao, Z. Guo, Deeply understanding the Zn anode behaviour and corresponding improvement strategies in different aqueous Zn-based batteries, Energy & Environmental Science 13(11) (2020) 3917-3949.
[15] L. Wang, M. Jia, X. Xu, Q. Wang, Asymmetric aqueous Zn-air battery with high voltage of 2.16 V by metal organic framework derived Co-Nx based bi-functional

electrocatalyst as cathode, J. Power Sources 437 (2019) 226892.
[16] Y. Huang, Z. Li, Z. Pei, Z. Liu, H. Li, M. Zhu, J. Fan, Q. Dai, M. Zhang, L. Dai, C. Zhi, Solid-State Rechargeable Zn//NiCo and Zn-Air Batteries with Ultralong Lifetime and High Capacity: The Role of a Sodium Polyacrylate Hydrogel Electrolyte, Advanced Energy Materials 8(31) (2018) 1802288.
[17] R. Chen, X. Xu, S. Peng, J. Chen, D. Yu, C. Xiao, Y. Li, Y. Chen, X. Hu, M. Liu, H. Yang, I. Wyman, X. Wu, A Flexible and Safe Aqueous Zinc–Air Battery with a Wide Operating Temperature Range from −20 to 70 °C, ACS Sustainable Chemistry & Engineering 8(31) (2020) 11501-11511.
[18] S. Zhao, Y. Zuo, T. Liu, S. Zhai, Y. Dai, Z. Guo, Y. Wang, Q. He, L. Xia, C. Zhi, Multi-Functional Hydrogels for Flexible Zinc-Based Batteries Working under Extreme Conditions, Advanced Energy Materials (2021) 2101749.
[19] H. Tang, Y. Yin, Y. Huang, J. Wang, L. Liu, Z. Qu, H. Zhang, Y. Li, M. Zhu, O.G. Schmidt, Battery-Everywhere Design Based on a Cathodeless Configuration with High Sustainability and Energy Density, ACS Energy Letters 6(5) (2021) 1859-1868.
[20] S. Zhao, K. Wang, S. Tang, X. Liu, K. Peng, Y. Xiao, Y. Chen, A new solid-state zinc–air battery for fast charge, Energy Technology 8(5) (2020) 1901229.
[21] C. Dai, X. Jin, H. Ma, L. Hu, G. Sun, H. Chen, Q. Yang, M. Xu, Q. Liu, Y. Xiao, Maximizing Energy Storage of Flexible Aqueous Batteries through Decoupling Charge Carriers, Advanced Energy Materials 11(14) (2021) 2003982.
[22] G.G. Yadav, D. Turney, J. Huang, X. Wei, S. Banerjee, Breaking the 2 V barrier in aqueous zinc chemistry: Creating 2.45 and 2.8 V MnO2–Zn aqueous batteries, ACS Energy Letters 4(9) (2019) 2144-2146.
[23] P. Tan, B. Chen, H. Xu, H. Zhang, W. Cai, M. Ni, M. Liu, Z. Shao, Flexible Zn– and Li–air batteries: recent advances, challenges, and future perspectives, Energy Environ. Sci. 10(10) (2017) 2056-2080.
[24] Y. Li, J. Fu, C. Zhong, T. Wu, Z. Chen, W. Hu, K. Amine, J. Lu, Recent Advances in Flexible Zinc-Based Rechargeable Batteries, Advanced Energy Materials 9(1) (2019) 1802605.
[25] S. Zhao, D. Xia, M. Li, D. Cheng, K. Wang, Y.S. Meng, Z. Chen, J. Bae, Self-Healing and Anti-CO2 Hydrogels for Flexible Solid-State Zinc-Air Batteries, ACS applied materials & interfaces (2021).
[26] J. Kestin, M. Sokolov, W.A. Wakeham, Viscosity of liquid water in the range− 8 C to 150 C, J. Phys. Chem. Ref. Data 7(3) (1978) 941-948.
[27] S. Siu, J. Evans, Density and viscosity measurements of zincate/KOH solutions, J. Electrochem. Soc. 144(4) (1997) 1278.
[28] X. Fan, J. Liu, Z. Song, X. Han, Y. Deng, C. Zhong, W. Hu, Porous nanocomposite gel polymer electrolyte with high ionic conductivity and superior electrolyte retention capability for long-cycle-life flexible zinc–air batteries, Nano Energy 56 (2019) 454-462.
[29] Q. Rong, W. Lei, L. Chen, Y. Yin, J. Zhou, M. Liu, Anti-freezing, Conductive Self-healing Organohydrogels with Stable Strain-Sensitivity at Subzero Temperatures, Angew. Chem. Int. Ed. Engl. 56(45) (2017) 14159-14163.
[30] J. Zhao, K.K. Sonigara, J. Li, J. Zhang, B. Chen, J. Zhang, S.S. Soni, X. Zhou, G.

Cui, L. Chen, A smart flexible zinc battery with cooling recovery ability, Angew. Chem. Int. Ed. 56(27) (2017) 7871-7875.
[31] D. Wang, H. Li, Z. Liu, Z. Tang, G. Liang, F. Mo, Q. Yang, L. Ma, C. Zhi, A Nanofibrillated Cellulose/Polyacrylamide Electrolyte-Based Flexible and Sewable High-Performance Zn-MnO2 Battery with Superior Shear Resistance, Small 14(51) (2018) e1803978.
[32] L. Ma, S. Chen, X. Li, A. Chen, B. Dong, C. Zhi, Liquid-Free All-Solid-State Zinc Batteries and Encapsulation-Free Flexible Batteries Enabled by In Situ Constructed Polymer Electrolyte, Angew. Chem. 132(52) (2020) 24044-24052.
[33] N. Vassal, E. Salmon, J.-F. Fauvarque, Electrochemical properties of an alkaline solid polymer electrolyte based on P (ECH-co-EO), Electrochim. Acta 45(8-9) (2000) 1527-1532.
[34] A. Mohamad, N. Mohamed, M. Yahya, R. Othman, S. Ramesh, Y. Alias, A. Arof, Ionic conductivity studies of poly (vinyl alcohol) alkaline solid polymer electrolyte and its use in nickel–zinc cells, Solid State Ionics 156(1-2) (2003) 171-177.
[35] J. Park, M. Park, G. Nam, J.s. Lee, J. Cho, All-solid-state cable-type flexible zinc–air battery, Adv. Mater. 27(8) (2015) 1396-1401.
[36] P. Cai, Y. Li, J. Chen, J. Jia, G. Wang, Z. Wen, An Asymmetric-Electrolyte Zn− Air Battery with Ultrahigh Power Density and Energy Density, ChemElectroChem 5(4) (2018) 589-592.
[37] J. Fu, D.U. Lee, F.M. Hassan, L. Yang, Z. Bai, M.G. Park, Z. Chen, Flexible high-energy polymer-electrolyte-based rechargeable zinc–air batteries, Adv. Mater. 27(37) (2015) 5617-5622.
[38] H. Miao, B. Chen, S. Li, X. Wu, Q. Wang, C. Zhang, Z. Sun, H. Li, All-solid-state flexible zinc-air battery with polyacrylamide alkaline gel electrolyte, J. Power Sources 450 (2020) 227653.
[39] Z. Pei, Z. Yuan, C. Wang, S. Zhao, J. Fei, L. Wei, J. Chen, C. Wang, R. Qi, Z. Liu, A Flexible Rechargeable Zinc–Air Battery with Excellent Low-Temperature Adaptability, Angew. Chem. 132(12) (2020) 4823-4829.
[40] Z. Pei, Y. Huang, Z. Tang, L. Ma, Z. Liu, Q. Xue, Z. Wang, H. Li, Y. Chen, C. Zhi, Enabling highly efficient, flexible and rechargeable quasi-solid-state zn-air batteries via catalyst engineering and electrolyte functionalization, Energy Storage Materials 20 (2019) 234-242.
[41] J. Liu, M. Hu, J. Wang, N. Nie, Y. Wang, Y. Wang, J. Zhang, Y. Huang, An intrinsically 400% stretchable and 50% compressible NiCo//Zn battery, Nano Energy 58 (2019) 338-346.
[42] Y. Bai, B. Chen, F. Xiang, J. Zhou, H. Wang, Z. Suo, Transparent hydrogel with enhanced water retention capacity by introducing highly hydratable salt, Appl. Phys. Lett. 105(15) (2014) 151903.
[43] X. Hu, Z. Ma, J. Li, Z. Cai, Y. Li, B. Zu, X. Dou, Superior water anchoring hydrogel validated by colorimetric sensing, Materials Horizons 7(12) (2020) 3250-3257.
[44] Y. Xu, P. Cai, K. Chen, Y. Ding, L. Chen, W. Chen, Z. Wen, High-Voltage Rechargeable Alkali–Acid Zn–PbO2 Hybrid Battery, Angew. Chem. 132(52) (2020) 23799-23803.

[45] C. Zhong, B. Liu, J. Ding, X. Liu, Y. Zhong, Y. Li, C. Sun, X. Han, Y. Deng, N. Zhao, Decoupling electrolytes towards stable and high-energy rechargeable aqueous zinc–manganese dioxide batteries, Nature Energy 5(6) (2020) 440-449.
[46] D. Jiao, Z. Ma, J. Li, Y. Han, J. Mao, T. Ling, S. Qiao, Test factors affecting the performance of zinc–air battery, Journal of Energy Chemistry 44 (2020) 1-7.
[47] S. Wu, Q. Zhang, J. Ma, D. Sun, Y. Tang, H. Wang, Interfacial design of Al electrode for efficient aluminum-air batteries: issues and advances, Materials Today Energy 18 (2020) 100499.